LUMPED EQUIVALENT MODELS OF COMPLEX RF STRUCTURES*

T. Flisgen†, J. Heller, U. van Rienen, Universität Rostock, IAE, IEF, 18059 Rostock, Germany

Abstract

The prediction of RF properties of complex accelerating structures is an important issue in computational accelerator physics. This paper describes the derivation of state space equations for complex structures based on real eigenmodes of sections of the decomposed complex structure. The state space equations enable the calculation of system responses due to port excitations by means of standard ordinary differential equation solvers. Therefore, the state space equations are referred to as lumped equivalent models of such complex RF structures. Besides fast computation of system responses, the equivalent models enable the calculation of secondary quantities such as external quality factors. The present contribution discusses theoretical aspects by means of a validation example.

INTRODUCTION

The investigation of complex radio frequency (RF) structures is a crucial task in the design of particle accelerators. Often the treatment of these complex and large RF devices exceeds the capabilities of modern workstation computers. Therefore, many problems are tackled by means of cluster computers in combination with suitable parallel simulation codes (e.g. ACE3P [1]). In this contribution a proof of principle for an alternative approach is presented. Here, the complex structure is decomposed into segments likewise it is proposed by the method of Coupled S-Parameter Calculations (CSC) [2, 3]. This decomposition has the following advantages:

- The separate treatment of the segments is less time- and memory-consuming.

- The properties of equal segments need to be computed only once.

- If sections show symmetries their treatment can be further simplified.

- If Maxwell's equations can be solved analytically for sections their numerical treatment is not needed.

- If parameter studies are of interest only the properties of sections with free parameter(s) need to be recalculated.

After decomposition of the complex structure, state space equations in an impedance formulation for the segments are created by a 3D eigenmode expansion [4, 5, 6]. These impedance state space equations are also referred to

as lumped equivalent models of the segments as they describe the dependency of the transient modal voltages on transient modal currents at the segment's waveguide ports. By employing a modification of the CSC scheme, the state equations of the segments are combined to obtain the state space equations of the complete structure. These equations allow for the computation of transient system responses as well as frequency domain transfer functions. Furthermore, secondary quantities such as external quality factors can be derived from the lumped model. In addition, the field distribution inside the full structure is also available as the state equations for the individual segments are obtained by a 3D eigenmode expansion.

In comparison to [6] where the coupling scheme is introduced and the focus lies on theoretical derivations, this paper presents a more sophisticated application example for the creation of lumped equivalent models of complex RF structures.

APPLICATION EXAMPLE AND CREATION OF ITS LUMPED MODEL

A third harmonic cavity with three cells (see [7] for geometric details) and simplified higher order mode (HOM) couplers[1] is chosen as an application example. The entire structure is considered to be lossless and the beam pipes are shortcut with perfect electric conducting (PEC) walls. Fig. 1 shows the structure under test and its decomposition into segments. The entire structure is comparably small and not complex such that the direct numerical calculation of its properties like the transfer function is easily feasible for the sake of comparison and validation. To model these sections, five different state space equations of the form

$$\frac{\partial}{\partial t}\mathbf{x}_r(t) = \mathbf{A}_r\,\mathbf{x}_r(t) + \mathbf{B}_r\,\mathbf{i}_r(t), \qquad (1)$$

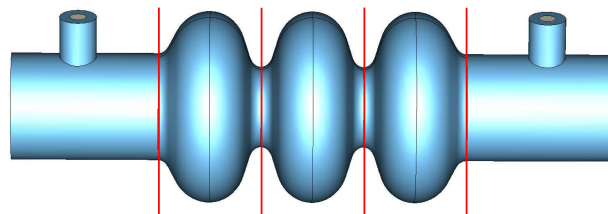$$\mathbf{v}_r(t) = \mathbf{B}_r^{\mathrm{T}}\,\mathbf{x}_r(t). \qquad (2)$$

Figure 1: Lossless third harmonic cavity with two end cells, one middle cell and two simplified HOM couplers and its decomposition into five segments (left coupler, left end cell, middle cell, right end cell and right coupler).

[1]An antenna tip protruding into the beam pipe.

are established. The matrix $\mathbf{A}_r$ is the state matrix, $\mathbf{B}_r$ the input matrix and $\mathbf{B}_r^{\mathrm{T}}$ the output matrix of the r-th section. The excitation term $\mathbf{i}_r(t)$ embraces the modal currents at the waveguide ports of the r-th segment and $\mathbf{v}_r(t)$ combines its modal voltages, respectively:

$$\mathbf{i}_r(t) = \begin{pmatrix} i_{r,1}(t) \\ i_{r,2}(t) \\ \vdots \\ i_{r,m}(t) \\ \vdots \\ i_{r,M_r}(t) \end{pmatrix} \text{ and } \mathbf{v}_r(t) = \begin{pmatrix} v_{r,1}(t) \\ v_{r,2}(t) \\ \vdots \\ v_{r,m}(t) \\ \vdots \\ v_{r,M_r}(t) \end{pmatrix}. \quad (3)$$

Here M_r denotes the number of total waveguide port modes of the section indexed by r.

The state matrices in (1) and (2) are obtained by a real eigenmode computation for each segment with perfect magnetic conducting (PMC) boundary conditions on the cross section of the waveguide ports and PEC boundary conditions on the remaining boundaries [4, 6]. In addition to the eigenfrequencies and modes, the impedance matrix of each segment is computed on 10 discrete frequency samples to calculate a correction term which accounts for non considered higher (or lower) order modes [4, 5, 6]. All computations are performed by CST Studio Suite® [8]. Hereinafter details on the individual calculations are presented.

State Space Matrices for HOM Coupler

Fig. 2 illustrates the left HOM coupler (segment index $r = 1$) and its network theoretical counterpart with the generalized voltages and currents of the respective waveguide modes. At the coaxial port of the coupler only the TEM mode is considered (port mode index $m = 1$), whereas 12 circular waveguide modes at the beam pipe are used for the concatenation (port mode indices $m = 2, \ldots, 13$). The HOM coupler is discretized exploiting its symmetry on a hexahedral mesh with $34,200$ mesh cells. Based on this meshing 50 eigenmodes are computed in combination with 10 impedance matrices sampled on discrete frequencies for the correction term. Furthermore, the field distributions of 13 2D port modes are determined by the CST Microwave Studio® frequency domain solver. Based on these calculations the matrices $\mathbf{A}_{HOM} \in \mathbb{R}^{151 \times 151}$ and $\mathbf{B}_{HOM} \in \mathbb{R}^{151 \times 13}$ are obtained (refer to (1) and (2)).

State Space Matrices for End and Middle Cell

Fig. 3 illustrates the end cell and its equivalent circuit diagram with generalized voltages and currents of the waveguide modes (the treatment of the middle cell is analogous). On both cut planes 12 port modes are used for the 2D field expansion. The end cell is discretized on a hexahedral mesh with $58,806$ mesh cells exploiting one symmetry plane (for the middle cell $39,600$ mesh cells are used). By employing this discretization 50 eigenmodes are computed in combination with 10 impedance matrices needed for the correction term. Furthermore, the field distributions of 24 2D
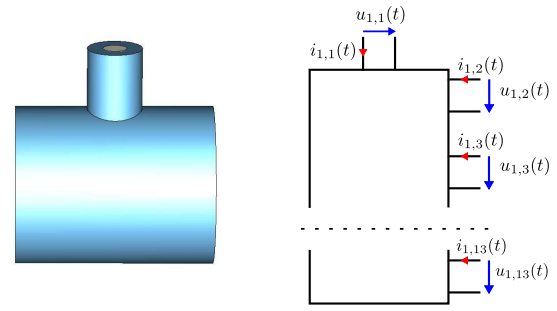

Figure 2: Lossless HOM coupler (left) and its equivalent circuit diagram (right) with indicated modal voltages (blue arrows) and currents (red arrows).

port modes (12 modes on each cut plane) are determined by the CST Microwave Studio® frequency domain solver. Based on these calculations the matrices for the endcells $\mathbf{A}_{ec} \in \mathbb{R}^{176 \times 176}$, $\mathbf{B}_{ec} \in \mathbb{R}^{176 \times 24}$ and for the midcells $\mathbf{A}_{mc} \in \mathbb{R}^{184 \times 184}$, $\mathbf{B}_{mc} \in \mathbb{R}^{184 \times 24}$ are obtained.
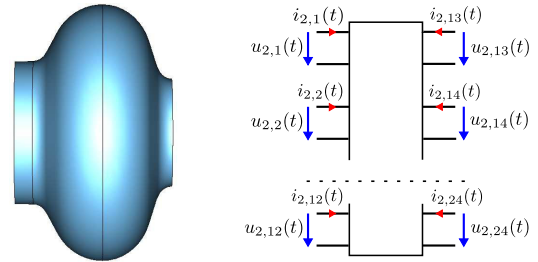

Figure 3: Lossless end cell (left) and its network theoretical counterpart (right) with the generalized voltages (blue arrows) and currents (red arrows).

Concatenation of the Sections

To obtain a lumped equivalent model of the complete structure, the state equations for the five individual segments are collected by the block system

$$\frac{\partial}{\partial t} \underbrace{\begin{pmatrix} \mathbf{x}_1(t) \\ \mathbf{x}_2(t) \\ \vdots \\ \mathbf{x}_5(t) \end{pmatrix}}_{\mathbf{x}_d(t)} = \underbrace{\begin{pmatrix} \mathbf{A}_1 & 0 & \ldots & 0 \\ 0 & \mathbf{A}_2 & \ldots & 0 \\ \vdots & \ldots & \ddots & \vdots \\ 0 & \ldots & \ldots & \mathbf{A}_5 \end{pmatrix}}_{\mathbf{A}_d} \underbrace{\begin{pmatrix} \mathbf{x}_1(t) \\ \mathbf{x}_2(t) \\ \vdots \\ \mathbf{x}_5(t) \end{pmatrix}}_{\mathbf{x}_d(t)}$$

$$+ \underbrace{\begin{pmatrix} \mathbf{B}_1 & 0 & \ldots & 0 \\ 0 & \mathbf{B}_2 & \ldots & 0 \\ \vdots & \ldots & \ddots & \vdots \\ 0 & \ldots & \ldots & \mathbf{B}_5 \end{pmatrix}}_{\mathbf{B}_d} \underbrace{\begin{pmatrix} \mathbf{i}_1(t) \\ \mathbf{i}_2(t) \\ \vdots \\ \mathbf{i}_5(t) \end{pmatrix}}_{\mathbf{i}_{can}(t)},$$

$$(4)$$

where $\mathbf{A}_1 = \mathbf{A}_5 = \mathbf{A}_{HOM}$, $\mathbf{A}_2 = \mathbf{A}_4 = \mathbf{A}_{ec}$, $\mathbf{A}_3 = \mathbf{A}_{mc}$, $\mathbf{B}_1 = \mathbf{B}_5 = \mathbf{B}_{HOM}$, $\mathbf{B}_2 = \mathbf{B}_4 = \mathbf{B}_{ec}$ and $\mathbf{B}_3 = \mathbf{B}_{mc}$. In the same manner, the output equations (2) are

combined for all sections:

$$
\begin{pmatrix} \mathbf{v}_1(t) \\ \mathbf{v}_2(t) \\ \vdots \\ \mathbf{v}_5(t) \end{pmatrix} = \underbrace{\begin{pmatrix} \mathbf{B}_1^T & \mathbf{0} & \dots & \mathbf{0} \\ \mathbf{0} & \mathbf{B}_2^T & \dots & \mathbf{0} \\ \vdots & \dots & \ddots & \vdots \\ \mathbf{0} & \dots & \dots & \mathbf{B}_5^T \end{pmatrix}}_{\mathbf{B}_d^T} \underbrace{\begin{pmatrix} \mathbf{x}_1(t) \\ \mathbf{x}_2(t) \\ \vdots \\ \mathbf{x}_5(t) \end{pmatrix}}_{\mathbf{x}_d(t)} . \quad (5)
$$
$$
\underbrace{\phantom{\begin{pmatrix} \mathbf{v}_1(t) \end{pmatrix}}}_{\mathbf{v}_{can}(t)}
$$

The resulting ordering of the currents $\mathbf{i}_{can}(t)$ and voltages $\mathbf{v}_{can}(t)$ is defined as <u>canonical</u> ordering. It is reordered by a permutation matrix $\mathbf{P}^T$ (one coefficient equal to one in each row and in each column, while the remaining coefficients are equal to zero) to sort for internal and external quantities:

$$
\mathbf{i}_{sort}(t) = \begin{pmatrix} \mathbf{i}_{int}(t) \\ \mathbf{i}_{ext}(t) \end{pmatrix} = \mathbf{P}^T \mathbf{i}_{can}(t), \quad (6)
$$

$$
\mathbf{v}_{sort}(t) = \begin{pmatrix} \mathbf{v}_{int}(t) \\ \mathbf{v}_{ext}(t) \end{pmatrix} = \mathbf{P}^T \mathbf{v}_{can}(t). \quad (7)
$$

Internal quantities belong to waveguide ports located at the decomposition planes and external ports are ports of the complete structure. Thus, the vectors $\mathbf{i}_{ext}(t)$ and $\mathbf{v}_{ext}(t)$ embrace the port quantities which belong to the $N_{ext} = 2$ external TEM ports located at the HOM antenna tips:

$$
\mathbf{i}_{ext}(t) = \begin{pmatrix} i_{1,1}(t) \\ i_{5,1}(t) \end{pmatrix} \text{ and } \mathbf{v}_{ext}(t) = \begin{pmatrix} v_{1,1}(t) \\ v_{5,1}(t) \end{pmatrix}. \quad (8)
$$

It is crucial to note, that vectors holding the internal quantities are organised such that quantities belonging to connected ports are listed pairwise below each other. E.g. for the connection between the left HOM coupler and the left end cell (see Fig. 4) this reads as

$$
\mathbf{i}_{int}(t) = \begin{pmatrix} i_{1,2}(t) \\ i_{2,1}(t) \\ i_{1,3}(t) \\ i_{2,2}(t) \\ \vdots \\ i_{1,13}(t) \\ i_{2,12}(t) \\ \vdots \end{pmatrix} \text{ and } \mathbf{v}_{int}(t) = \begin{pmatrix} v_{1,2}(t) \\ v_{2,1}(t) \\ v_{1,3}(t) \\ v_{2,2}(t) \\ \vdots \\ v_{1,13}(t) \\ v_{2,12}(t) \\ \vdots \end{pmatrix}. \quad (9)
$$

By employment of the orthogonality of the permutation matrix $\mathbf{P}^T = \mathbf{P}^{-1}$ the canonical quantities in (4) and (5) are replaced by the sorted quantities:

$$
\frac{\partial}{\partial t} \mathbf{x}_d(t) = \mathbf{A}_d \mathbf{x}_d(t) + \underbrace{\mathbf{B}_d \mathbf{P}}_{\bar{\mathbf{B}}_d} \mathbf{i}_{sort}(t), \quad (10)
$$

$$
\mathbf{v}_{sort}(t) = \underbrace{\mathbf{P}^T \mathbf{B}_d^T}_{\bar{\mathbf{B}}_d^T} \mathbf{x}_d(t). \quad (11)
$$

To split these equations into internal and external quantities, the matrix $\bar{\mathbf{B}}_d$ is partitioned:

$$
\bar{\mathbf{B}}_d = \begin{pmatrix} \bar{\mathbf{B}}_{d1} & \bar{\mathbf{B}}_{d2} \end{pmatrix}, \quad (12)
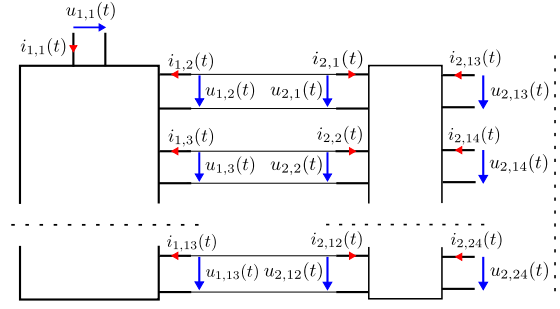$$

Figure 4: Equivalent circuit diagram of the concatenation between the left HOM coupler and the right end cell.

where $\bar{\mathbf{B}}_{d1}$ has $N_{int} = 96$ columns and $\bar{\mathbf{B}}_{d2}$ has $N_{ext} = 2$ columns. Utilizing this together with (10) and (11) leads to

$$
\frac{\partial}{\partial t} \mathbf{x}_d(t) = \mathbf{A}_d \mathbf{x}_d(t) + \bar{\mathbf{B}}_{d1} \mathbf{i}_{int}(t) + \bar{\mathbf{B}}_{d2} \mathbf{i}_{ext}(t), \quad (13)
$$

$$
\mathbf{v}_{int}(t) = \bar{\mathbf{B}}_{d1}^T \mathbf{x}_d(t), \quad (14)
$$

$$
\mathbf{v}_{ext}(t) = \bar{\mathbf{B}}_{d2}^T \mathbf{x}_d(t). \quad (15)
$$

Obviously, (15) is the output equation of the concatenated structure since it describes the relationship between the inner states and the external voltages.

To derive the corresponding state equation of the concatenated structure, the following two requirements are used. First, currents of terminals connected to each other have the same magnitude but a different sign (see e.g. $i_{1,2}(t) = -i_{2,1}(t)$ or $i_{1,3}(t) = -i_{2,2}(t)$ in Fig. 4). Second, they are listed pairwise below each other. In consequence, the N_{int} internal currents are expressed by

$$
\mathbf{i}_{int}(t) = \mathbf{F} \hat{\mathbf{i}}_{int}(t), \quad (16)
$$

where

$$
\mathbf{F} = \text{diag}\left(\begin{pmatrix} 1 \\ -1 \end{pmatrix}, \dots, \begin{pmatrix} 1 \\ -1 \end{pmatrix} \right) \in \mathbb{R}^{N_{int} \times N_{int}/2}. \quad (17)
$$

The vector $\hat{\mathbf{i}}_{int}(t) \in \mathbb{R}^{N_{int}/2}$ contains the independent currents flowing through the coupled ports. Replacing (16) in (13) yields

$$
\frac{\partial}{\partial t} \mathbf{x}_d(t) = \mathbf{A}_d \mathbf{x}_d(t) + \bar{\mathbf{B}}_{d1} \mathbf{F} \hat{\mathbf{i}}_{int}(t) + \bar{\mathbf{B}}_{d2} \mathbf{i}_{ext}(t). \quad (18)
$$

The facts that voltages of connected terminals are equal (see e.g. $u_{1,2}(t) = u_{2,1}(t)$ or $u_{1,3}(t) = u_{2,2}(t)$ in Fig. 4) and that they are ordered below each other in $\mathbf{v}_{int}(t)$ yields

$$
\mathbf{F}^T \mathbf{v}_{int}(t) = \mathbf{F}^T \bar{\mathbf{B}}_{d1}^T \mathbf{x}_d(t) = \mathbf{0}. \quad (19)
$$

Multiplying (18) from left with $\mathbf{F}^T \bar{\mathbf{B}}_{d1}^T$ gives

$$
\frac{\partial}{\partial t} \underbrace{\mathbf{F}^T \bar{\mathbf{B}}_{d1}^T \mathbf{x}_d(t)}_{\mathbf{0}} = \mathbf{0} = \mathbf{F}^T \bar{\mathbf{B}}_{d1}^T \mathbf{A}_d \mathbf{x}_d(t)
$$
$$
+ \mathbf{F}^T \bar{\mathbf{B}}_{d1}^T \bar{\mathbf{B}}_{d1} \mathbf{F} \hat{\mathbf{i}}_{int}(t) + \mathbf{F}^T \bar{\mathbf{B}}_{d1}^T \bar{\mathbf{B}}_{d2} \mathbf{i}_{ext}(t) \quad (20)
$$

which is solved for the independent currents

$$\hat{\mathbf{i}}_{int}(t) = - \left[\mathbf{F}^{\mathrm{T}}\bar{\mathbf{B}}_{d1}^{\mathrm{T}}\bar{\mathbf{B}}_{d1}\mathbf{F}\right]^{-1}\mathbf{F}^{\mathrm{T}}\bar{\mathbf{B}}_{d1}^{\mathrm{T}}\mathbf{A}_d\,\mathbf{x}_d(t)$$
$$- \left[\mathbf{F}^{\mathrm{T}}\bar{\mathbf{B}}_{d1}^{\mathrm{T}}\bar{\mathbf{B}}_{d1}\mathbf{F}\right]^{-1}\mathbf{F}^{\mathrm{T}}\bar{\mathbf{B}}_{d1}^{\mathrm{T}}\bar{\mathbf{B}}_{d2}\,\mathbf{i}_{ext}(t). \quad (21)$$

Substituting the internal currents in (18) leads to the state equation of the concatenated structure

$$\frac{\partial}{\partial t}\mathbf{x}_d(t) = \mathbf{K}\left[\mathbf{A}_d\,\mathbf{x}_d(t) + \bar{\mathbf{B}}_{d2}\,\mathbf{i}_{ext}(t)\right], \quad (22)$$

with the idempotent and symmetric matrix

$$\mathbf{K} = \left[\mathbf{I} - \bar{\mathbf{B}}_{d1}\mathbf{F}\left[\mathbf{F}^{\mathrm{T}}\bar{\mathbf{B}}_{d1}^{\mathrm{T}}\bar{\mathbf{B}}_{d1}\mathbf{F}\right]^{-1}\mathbf{F}^{\mathrm{T}}\bar{\mathbf{B}}_{d1}^{\mathrm{T}}\right]. \quad (23)$$

To delete N_{int} redundant states in $\mathbf{x}_d(t)$, which result from the algebraic side constraint (19), the orthonormal basis of the kernel of $\mathbf{F}^{\mathrm{T}}\bar{\mathbf{B}}_{d1}^{\mathrm{T}}$

$$\mathbf{Q} = \mathrm{Ker}\left(\mathbf{F}^{\mathrm{T}}\bar{\mathbf{B}}_{d1}^{\mathrm{T}}\right), \text{ with } \mathbf{Q}^{\mathrm{T}}\mathbf{Q} = \mathbf{I} \quad (24)$$

is determined. By substituting

$$\mathbf{x}_d(t) = \mathbf{K}\mathbf{Q}\,\mathbf{x}_c(t) = \mathbf{Q}\,\mathbf{x}_c(t) \quad (25)$$

in (22) and (15) the redundant states vanish and a symmetric state space system of the concatenated structure is obtained:

$$\frac{\partial}{\partial t}\mathbf{x}_c(t) = \underbrace{\mathbf{Q}^{\mathrm{T}}\mathbf{K}\mathbf{A}_d\mathbf{K}\mathbf{Q}}_{\mathbf{A}_c}\,\mathbf{x}_c(t) + \underbrace{\mathbf{Q}^{\mathrm{T}}\mathbf{K}\bar{\mathbf{B}}_{d2}}_{\mathbf{B}_c}\,\mathbf{i}_{ext}(t), \quad (26)$$

$$\mathbf{v}_{ext}(t) = \underbrace{\bar{\mathbf{B}}_{d2}^{\mathrm{T}}\mathbf{K}\mathbf{Q}}_{\mathbf{B}_c^{\mathrm{T}}}\,\mathbf{x}_c(t). \quad (27)$$

RESULTS

In the following subchapters different quantities are computed by means of the created lumped model and are compared with direct computations.

Scattering Parameters

The impedance formulation (26) and (27) can be easily transferred to a scattering formulation assuming the external port impedances to be constant [6]:

$$\frac{\partial}{\partial t}\mathbf{x}_c(t) = \underbrace{\left(\mathbf{A}_c - \mathbf{B}_c\mathbf{D}_Z^{-1}\mathbf{B}_c^{\mathrm{T}}\right)}_{\mathbf{A}_{sc}}\,\mathbf{x}_c(t)$$
$$+ \underbrace{\sqrt{2}\,\mathbf{B}_c\mathbf{D}_Z^{-\frac{1}{2}}}_{\mathbf{B}_{sc}}\,\mathbf{a}(t) \quad (28)$$

and

$$\mathbf{b}(t) = \underbrace{\left(\sqrt{2}\,\mathbf{D}_Z^{-\frac{1}{2}}\mathbf{B}_c^{\mathrm{T}}\right)}_{\mathbf{B}_{sc}^{\mathrm{T}}}\,\mathbf{x}_c(t) + \underbrace{\left(-\mathbf{I}\right)}_{\mathbf{D}_{sc}}\,\mathbf{a}(t), \quad (29)$$

where the matrix $\mathbf{D}_Z$ holds the constant port impedances of the external ports on its main diagonal:

$$\mathbf{D}_Z = \mathrm{diag}\left(Z_1, Z_2\right). \quad (30)$$

The corresponding frequency domain transfer function is given by

$$\underline{\mathbf{b}}(j\omega) = \underbrace{\left[\mathbf{B}_{sc}^{\mathrm{T}}\left(j\omega\,\mathbf{I} - \mathbf{A}_{sc}\right)^{-1}\mathbf{B}_{sc} + \mathbf{D}_{sc}\right]}_{\underline{\mathbf{S}}(j\omega)}\underline{\mathbf{a}}(j\omega). \quad (31)$$

This transfer function is commonly known as the S-matrix[2] of the full structure. This matrix is evaluated in an interval $\Delta f = 3\ldots 8\,\mathrm{GHz}$ on $1,001$ discrete frequency samples. In contrast, the scattering properties of the complete structure are computed by means of a hexahedral discretization ($192,456$ mesh cells) in combination with the CST Microwave Studio® Fast S-parameter Solver [8]. Fig. 5 and Fig. 6 show the magnitude and the phase of the transmission between the external ports obtained by the concatenation scheme and by the full calculation.
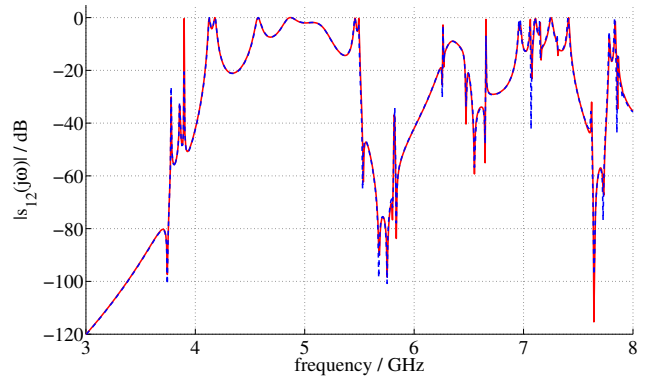

Figure 5: Absolute value of the transmission coefficient from left to right HOM coupler obtained by the concatenation scheme (red) and by direct calculation (blue).
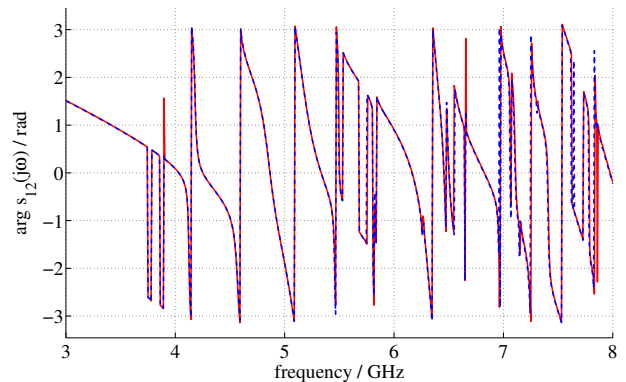

Figure 6: Phase of the transmission coefficient from left to right HOM coupler. The red curve is obtained by the concatenation scheme and the blue curve by direct calculation.

---

[2]In contrast to [2, 3] this matrix is not a priori sampled on discrete frequency points but is available in terms of an analytic function [6].

External Quality Factors

A typical quantity of interest in accelerator design is the external quality factor of modes inside the cavity structure:

$$Q_{ext,\nu} = \frac{\omega_\nu W_{stored,\nu}}{P_{ports,\nu}}. \qquad (32)$$

Here ω_ν is the angular frequency of the ν-th mode, $W_{stored,\nu}$ the energy stored in the ν-th mode and $P_{ports,\nu}$ the averaged loss power of the ν-th mode due to energy propagation through the external ports. The external quality factor can be computed by the lumped model via

$$Q_{ext,\nu} = \frac{\mathrm{Im}(\lambda_\nu)}{2\mathrm{Re}(\lambda_\nu)}, \qquad (33)$$

where λ_ν are the eigenvalues of the scattering formulation state matrix $\mathbf{A}_{sc}$. To benchmark the values computed by the concatenation scheme in combination with the upper equations, the eigenmode solver of CST Microwave Studio® is used to directly calculate external quality factors of the complete structure. In Fig. 7 the comparison for the modes in the interval Δf is given.
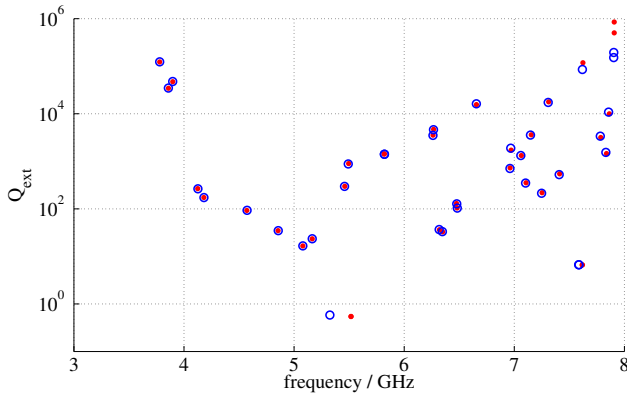

Figure 7: External quality factors of the structure under test in the interval Δf. The red dots are computed by the concatenation scheme, whereas the blue dots are computed by a direct calculation.

Transient System Responses

Often in accelerator design the response of complex structures due to different transient excitation signals is of interest (e.g. for the analysis of field filling and defilling processes). Once it is established, the state space system (28) and (29) allows for the computation of these responses using ordinary differential equation (ODE) solvers. Fig. 8 plots the transmitted signal at the right HOM coupler of the example structure due to the sinusoidal excitation

$$a_1(t) = \Big(1 - \exp(-t/T_r)\Big)\sin(2\pi f_0\, t) \qquad (34)$$

at the left coupler, where $f_0 = 3.8976\,\mathrm{GHz}$ and $T_r = 1\,\mathrm{ns}$. The red curve is obtained by the established lumped model in combination with an ODE solver and the blue curve is determined by the CST Microwave Studio® transient solver [8].
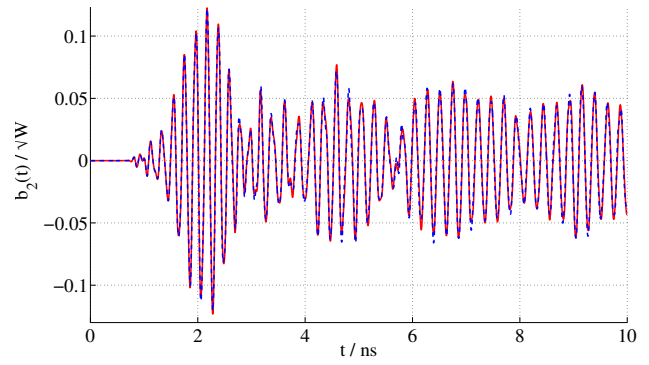

Figure 8: Transmitted signals $b_2(t)$ observed in right coupler due to excitation $a_1(t)$ at the left coupler. The red curve is obtained by the lumped model, whereas the blue curve is calculated with CST's transient solver.

CONCLUSIONS

The actual contribution presents a proof of concept for a method to create lumped equivalent models of complex RF structures. Based on a set of 3D eigenmodes of sections of the decomposed structure, state space equations are created. These equations are linked together to obtain a lumped equivalent model of the complete structure. This lumped model allows for the computation of complex structure's transfer function, transient system responses or secondary quantities. The validation example given in this paper shows that the model approximates the physical properties of the full structure in a very reasonable manner.

ACKNOWLEDGEMENTS

REFERENCES

[1] https://www.slac.stanford.edu/grp/acd/ace3p.html

[2] K. Rothemund et al., "Eigenmode Calculation in Long and Complex RF Structures Using the Coupled S-Parameter Calculation Technique," TESLA-REPORT 2000-33.

[3] H.-W. Glock et al., "CSC - A Procedure for Coupled S-Parameter Calculations," IEEE Trans. Magn. Vol. 38, 2002.

[4] M. Dohlus et al., "Calculation of Frequency Domain Parameters using 3D Eigensolutions", International Journal of Numerical Modelling Vol. 12, 1999.

[5] T. Wittig et al., "Model Order Reduction for Large Systems in Computational Electromagnetics," LinAlgApp 415, Special Issue on Order Reduction of Large-Scale Systems, 2006.

[6] T. Flisgen et al., "Lumped Equivalent Models of Complex RF Structures based on Segment's Eigenmodes," Paper draft to be submitted to the IEEE.

[7] T. Khabibouline et al., "Higher Order Modes of a 3rd Harmonic Cavity with an Increased End-cup Iris," TESLA-REPORT 2003-01, DESY, Hamburg 2003.

[8] CST Studio Suite®, CST AG, 64289 Darmstadt, Germany.